Available online at www.sciencedirect.com

ScienceDirect

Advances in Space Research 69 (2022) 2142–2157

ADVANCES IN SPACE RESEARCH
(a COSPAR publication)

www.elsevier.com/locate/asr

An audit of geomagnetic field in polar and south atlantic anomaly regions over two centuries

Amar Kakad *, Bharati Kakad

Indian Institute of Geomagnetism, New Panvel (West), Navi Mumbai, India

Received 27 June 2021; received in revised form 1 December 2021; accepted 5 December 2021
Available online 10 December 2021

Abstract

There are several reports about the decrease of the magnetic field of our planet. Here, we present a detailed investigation of the geomagnetic field over past 200 years using magnetic field models (IGRF+gufm1) and ground magnetic field observations until 2020. There are two prominent regions of consistently decreasing geomagnetic field namely: the South Atlantic Anomaly (SAA) and the southern pole region. The SAA region with field decreasing at 30 nT/year drifting to the south-west, whereas, the southern pole region with field decreasing at the rate 13 nT/year steadily drifting to the north-west. The Earth's polar (66°–90°) magnetic field was invariably higher around the south pole as compared to the field around the north pole. However, it is found that over the past few decades (since 1950), the average magnetic field in the southern polar region has decreased to such an extent that presently it is weaker than the northern polar magnetic field. This tendency of cross-over in the magnitudes of average polar magnetic field strength is also evident in the ground magnetic field observations. On the ground at Hermanus (station in the SAA region), the rate of decrease of the magnetic field is found to be much higher (98 nT/year) during 1950–2020. Such a significant decrease in the magnetic field at Hermanus could be associated with the splitting of the SAA as it is situated close to the second minima in the SAA region. It is found that the magnetic field gradients around the center of the SAA become shallower as we move towards the higher altitudes. Also, the center of the SAA steadily moves in the north-east direction with increasing altitude. Though the weakening of the geomagnetic field is not an impulsive phenomenon but can invoke serious concerns to our life, satellites, and climate in near future.

Keywords: Geomagnetic field; South atlantic anomaly; Polar geomagnetic field; Satellite and climate

1. Introduction

Our planet Earth possesses a strong magnetic field that is originated from its fluid outer core. This intrinsic field accounts for more than 95% of the magnetic energy of the observed magnetic field on the Earth's surface, generated by the process known as the Geodynamo. The magnetic field changes slowly on different timescales throughout geological history, which reflects changes deep within the Earth. This field has fundamental importance as it acts like a protective magnetic shield around the planet Earth, which safeguards its inhabitants from harmful highly energetic particles emitted from the Sun that can cause damage to living organisms, orbiting satellites, astronauts, and spacecrafts (Tsurutani et al., 2003). At the same time, some of the charged particles that manage to enter the Earth's magnetosphere get trapped along magnetic field lines and they are responsible for the generation of intense electric currents in the Earth's upper atmosphere (Kakad et al., 2019; Kakad and Kakad, 2020), which in turn can damage our power systems (Molinski et al., 2000). It is shown that long-term changes in the Earth's climate are

* Corresponding author.
E-mail addresses: amar.kakad@iigm.res.in (A. Kakad), bharati.kakad@iigm.res.in (B. Kakad).

https://doi.org/10.1016/j.asr.2021.12.011
0273-1177/

controlled by the cosmic ray flux (Lanci et al., 2020). The Earth's magnetic field can potentially control the cosmic rays entering the Earth. It is suggested that the geomagnetic field is an important driving component to the variations of the climate (Campuzano et al., 2018). Therefore, the need for understanding the behavior of the Earth's magnetic field variations is becoming ever more important in modern times.

Among the behavioural changes of the geomagnetic field, the changes in the South Atlantic regions and the geomagnetic polar regions are the main concerns raised by several recent studies (Hartmann and Pacca, 2009; Pavon-Carrasco and De Santis, 2016; Brown et al., 2018). The South Atlantic Anomaly (SAA) is a region on the Earth's surface where the intensity of the magnetic field is much weaker than elsewhere across the globe. This region is known to be continuously growing in extent and moving westward from the equator to southern latitudes (Campuzano et al., 2019; Amit et al., 2021). It is suggested that the conditions at the core-mantle boundary related to long-lived structures such as the Large Low Shear Velocity Provinces (LLSVPs) below southern Africa (Garnero and McNamara, 2008) may be responsible for the formation of anomaly regions like SAA (Tarduno et al., 2015). The LLSVPs in the lowermost mantle are key to understand the chemical composition and thermal structure of the deep Earth, but their origins have long been debated (Wang et al., 2021). Some researchers believe that the decrease in the magnetic field inside the SAA might have a link to the geomagnetic pole reversals (Tarduno et al., 2015; Brown et al., 2018). The behaviour of the polar cap during the magnetic field reversal has been modelled and it suggests that during such reversals the auroral zones may reach mid- and low-latitude regions, also the atmosphere may become more vulnerable due to the direct entry of energetic particles into the atmosphere (Zossi et al., 2019). Such an area of low magnetic field intensity is so pronounced that it allows cosmic rays, and energetic particles of Earth's inner radiation belts to reach much lower altitudes than at similar latitudes around the globe (Schaefer et al., 2016; Domingos et al., 2017). This leads to an increased flux of energetic particles in this region and exposes orbiting satellites to higher-than-usual levels of radiation. The long-term feature of Earth's internal magnetic field shows a decreasing trend in the SAA region. This will have major consequences for the operation and protection of surface instruments and satellites over the SAA region. Therefore, understanding the temporal and spatial variations of the geomagnetic field over the SAA region is one of the most active Earth research problems.

The Earth's magnetic field in the polar regions as well plays a crucial role in the terrestrial phenomena link to magnetic poles. Recently, Girgis et al., 2020 suggested that both south and north magnetic poles could be main drivers of SAA magnetic field response, resulting from the space weather conditions. A rapid decrease in the total magnetic field at Antarctic stations has been reported earlier (Rajaram et al., 2002; Cafarella et al., 2009). Such a decrease in the magnetic field is an alarming situation for our space weather and climate. It is because then polar cap and auroral regions will experience frequent precipitation of energetic particles. The wider exposure of the atmosphere to energetic particles and the enhanced precipitation due to the weakening of the polar magnetic field can modify global neutral wind and temperature patterns. In general, we are aware that the Earth's magnetic field is decreasing (Gubbins et al., 2006; Finlay, 2008; Finlay et al., 2012). However, its long-term forecast is difficult due to the complexities involved in the internal geodynamo process. On larger time scales, it is the main driver to control the SAA features like rate of decrease of the magnetic field, latitudinal-longitudinal coverage. The possibility of splitting of SAA is reported in a recent study (Rother et al., 2021). Therefore, to understand the present scenario the continuous monitoring and scrutiny of this weakening of the geomagnetic field is essential. Although, in earlier studies geomagnetic field variations have been examined for 1590–2005, here we present a detailed audit of the geomagnetic field of the polar and south Atlantic anomaly regions using the model and ground magnetic field observations by taking into account the variations in the recent years. It will help us to improve our understanding about the most recent features of variations in geomagnetic fields. The article is structured as follows. The data and model used in the present study are described in Section 2. Results are presented and discussed in Section 3. The present study is summarized and concluded in Section 4.

2. Data and methodology

In the present study, we have used the geomagnetic field calculator available at www.ngdc.noaa.gov/geomag, which provides the Earth's total magnetic field strength during the period 1590–2020. This calculator uses the thirteenth generation of the International Geomagnetic Reference Field (IGRF-13) model (Alken et al., 2021a; Alken et al., 2021b) to obtain the Earth's magnetic field for the period 1900–2020. From 1590 to 1900, this calculator uses the geomagnetic field based on the gufm1 model (Jackson et al., 2000). The gufm1 model is a geomagnetic field model based on historical geomagnetic data covering the period 1590–1990 (Jackson et al., 2000). Furthermore, a smooth transition from gufm1 to IGRF is imposed in the calculator from 1890 to 1900. In the present study, initially, the geomagnetic field strength on the surface of the Earth (Height, $H = 0$ km) is obtained at the interval of every 5 years by taking the grid of 1° in the latitudinal and longitudinal direction for the period of 1590–2020. In addition, for the years 1900 and 2020, we obtained the geomagnetic field strength at different altitudes above the surface of the Earth. The altitudes are considered in the range of 0–5000 km at an interval of 200 km. The magnetic field intensities estimated from the gufm1 model are not well constrained before 1840. Due to the unavailability of historical magnetic field data, the gufm1 model magnetic field values before 1840 are based on the linear extrapolation of the first Gauss coefficient g01 according to its evolution during the most recent epochs, 1840–1990 (Pavon-Carrasco and De Santis, 2016). Consequently, the results based on such extrapolated values are expected to have errors. Therefore, although we estimate geomagnetic field from 1590, we have used the magnetic field values only from 1840–2020 particularly to examine and quantify the movement, rate of decrease of the magnetic field, latitudinal and longitudinal extent for the SAA and polar regions of the Earth and their altitudinal variation. Besides, we used the ground magnetic field data from 15 observatories that cover the northern and southern polar regions (60°-90°) and the region of the SAA as per their availability. The details of these ground observatories are given in Table 1. The annual mean of the geomagnetic field recorded at these ground observatories is provided by the British Geological Survey, and it is available at http://www.geomag.bgs.ac.uk.

Before we proceed with the analysis, it is important to discuss the limitation of the gufm1 and IGRF models. For any empirical model, the accuracy of the model depends upon the spatio-temporal resolution of the observations considered in that model. The IGRF model describes the main geomagnetic field which is produced by internal sources primarily, inside the Earth's core. The model is valid on and above the Earth's surface, where the main geomagnetic field can be described as the gradient of a scalar potential. This scalar potential is represented as a finite series expansion in terms of the spherical harmonic coefficients, also known as the Gauss coefficients. As the geomagnetic field changes with time, a set of coefficients is specified every 5 years, with linear interpolation used for intermediate times. Therefore, to derive the accurate coefficients, we need global data coverage for all the relevant epochs. However, due to the absence of such ideal data, the estimated coefficients can have some errors (Lowes, 2000; Finlay et al., 2010b; Finlay et al., 2010a). In earlier versions of the IGRF model, the maximum spherical harmonic degree of expansion was chosen to be 10 up to epoch 1995. However, this has increased to 13 in the IGRF-13 model to account for the smaller scale internal signals, which can be captured by high-resolution satellite missions such as Ørsted, CHAMP and Swarm (Alken et al., 2021b). Thus, compared to previous models, IGRF-13 has paved the way for examining the secular variation of the geomagnetic field in the regions like SAA and Polar Regions more accurately. Thus, the main field obtained from the IGRF-13 and the ground station mostly follows the same trend. Nevertheless, it can have some uncertainties in the magnitude of the main field as compared to the ground observations, where the observational coverage is limited.

We tracked the variation of the minimum magnetic field B_{min} on the surface of the Earth and B_{max} from both polar regions since 1590 (see Supplementary Video S1). This video shows the variation of Earth's surface magnetic field during 1590–2020. We have marked the minimum magnetic field (B_{min}) with a white dot, the maximum magnetic field in the southern polar region (B^S_{max}) with a black asterisk and the maximum magnetic field in the northern polar region (B^N_{max}) with a black triangle. It may be noted that the maximum magnetic field on the entire globe (B_{max}) invariably lies in the southern polar region. In other words, the B_{min} and B_{max} falls in the SAA and southern pole region, respectively. The movement of the white dot and black asterisk clearly indicates the steady trajectory of these two regions on the surface of Earth during 1590–2020. However, for the northern pole region such consistent behaviour is not seen. Unlike SAA and the southern pole regions, the location of B^N_{max} is not stable. In the next section, we present some features related to the evolution of the geomagnetic field in the SAA and both polar regions.

Table 1
Details of 15 ground magnetic observatories in the Earth's polar and SAA regions that are used in the present study.

Regions	Observatory [Abbreviation]	Latitude [deg]	Longitude [deg]
SAA region	[1] Apia [API]	−13.80	−171.77
[Group-A]	[2] Hermanus [HER]	−34.42	19.23
Southern hemisphere	[1] Mawson [MAW]	−67.60	62.88
[Group-B]	[2]Vostok [VOS]	−78.45	106.86
	[3] Syowa [SYO]	−69.00	39.58
	[4] Scott-base [SBA]	−77.85	166.76
	[5] Dumont [DRV]	−66.66	140.0
Nothern hemisphere	[1] Dombas [DOB1–2]	62.06	9.10
[Group-C]	[2] Abisko [ABK]	68.35	18.82
	[3]Dikson Island [DIK]	73.54	80.56
	[4] Sodankyla [SOD]	67.46	26.60
	[5]Leirvogur [LRV]	64.18	−21.7
	[6] Yellowknife [YKC]	62.48	−114.48
	[7]Fort Churchill [FCC]	58.75	−94.08
	[8]Narsarsuaq [NAQ]	61.16	−45.44

3. Results and discussion

3.1. General features

The Earth's large-scale magnetic field varies over a longer time scale known as secular variation. To understand the global variation in the magnetic field, we obtained the Earth's surface magnetic field using the (IGRF+gufm1) model during 1590–2020 at every 5 years of interval. This magnetic field is a function of geographic latitude ($\lambda = -90^\circ$ to 90°), geographic longitude ($\phi = -180^\circ$ to -180°), time and altitude. We obtained the latitude (λ) and longitude (ϕ) of (i) the minimum magnetic field and (ii) the maximum magnetic field in the northern and southern hemisphere on the surface of the Earth and at an altitude of 1000 km for the period of 1590–2020. The minimum magnetic field is always located in the SAA region and the maximum magnetic field is located in the southern polar region. The variation of the minimum magnetic field B_{min}, its associated latitude λ_{min}, and longitude ϕ_{min} are shown in Fig. 1(a), (b) and (c), respectively for altitudes 0 km (black cross) and 1000 km (black dots). In each subplot, the gray patch represents the period of 1590–1840, where the modelled magnetic field values are based on the extrapolated value of the first gauss coefficient as no magnetic field data was available before 1840. Therefore, as seen in Fig. 1, while getting the trends by applying the least square fit we have utilized the data only after 1840. In Fig. 1(a) it is clearly seen that the magnetic field in the SAA region is continuously decreasing and the average rate of decrease is 30 nT/year and 19 nT/year at surface and at an altitude of 1000 km, respectively. Fig. 1(a) and (b) indicate the latitudinal and longitudinal movement of the minima. This minima has moved southward from approximately 19°S to 25°S in latitudes (see Fig. 1b), and westward from 20°W to 55°W in longitudes (see Fig. 1c). The southward shift in the latitude of 0.03°/year and the westward shift in the longitude of 0.22°/year are clearly evident during 1840–2020. However, at 1000 km, the minima in the SAA region is situated slightly north-east direction as compared to its location on the Earth's surface. On the surface, the B_{min} is located at 21°S,37°W, whereas at 1000 km it is located at 17°S,34°W. At an altitude of 1000 km, the south-west movement of minima is slow. It has moved southward from approximately 15°S to 19°S in latitudes, and westward from 16°W to 57°W in longi-

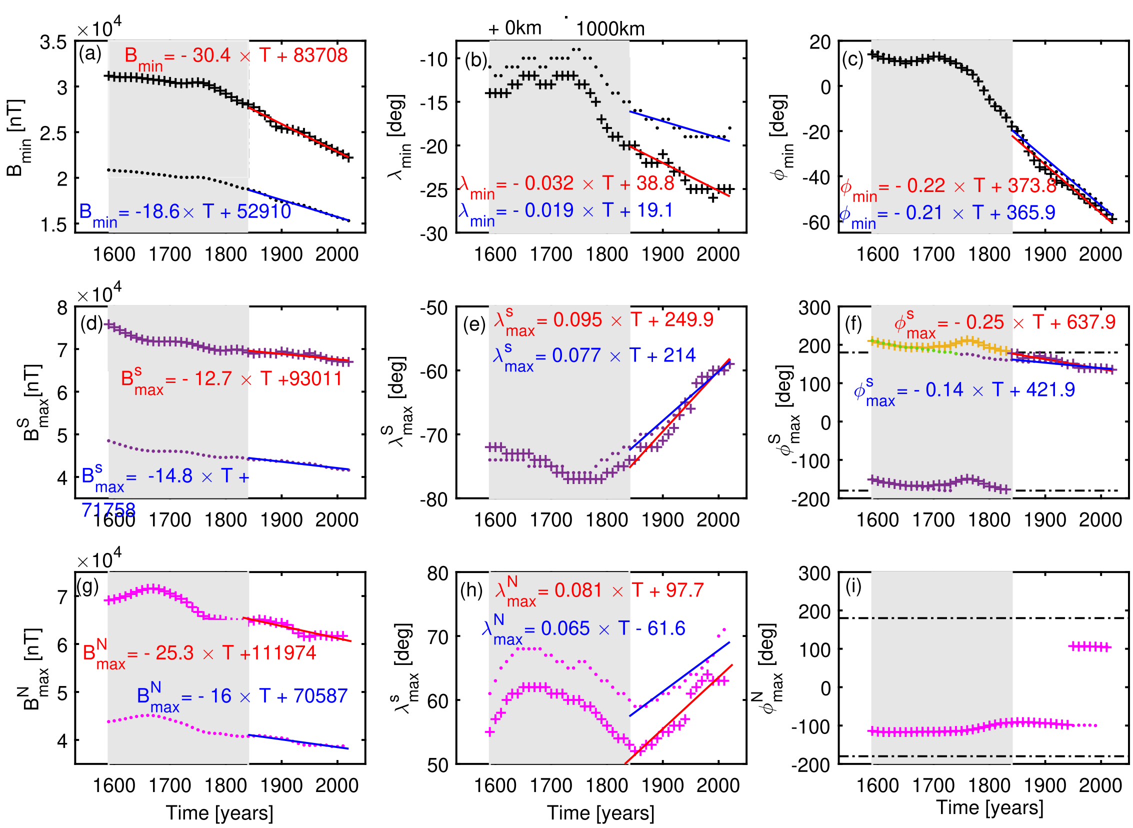

Fig. 1. This figure shows the variation of minimum magnetic field strength and associated latitude and longitude as a function of time in (a), (b), and (c), respectively. Similarly, variation of southern and northern hemisphere maximum magnetic field strength and associated latitude and longitude as a function of time in (d), (e), (f) and (g), (h), (i), respectively. These variations are shown for 0 km and 1000 km altitude from the surface of the Earth. The gray patch represents the period of 1590–1840, where the modelled magnetic field values are based on the extrapolated value of the first gauss coefficient as no magnetic field data was available before 1840. The variations from 1840–2020 are fitted with the least square and their equations are mentioned in respective subplots. The linear least square fits are shown with red line (0 kms) and black line (1000 km) in respective subplots.

tudes during 1840–2020, which implies that the southward shift in the latitude is 0.02°/year and the westward shift in longitude is 0.21°/year at an altitude of 1000 km.

The variation of maximum magnetic field from southern polar region (B^S_{max}) and their corresponding latitude λ^S_{max} and longitude ϕ^S_{max} are plotted as a function of time in Fig. 1(d), (e) and (f), respectively for altitude of 0 km and 1000 km. Similarly, for the northern polar region these parameters are plotted in Fig. 1(g), (h) and (i), respectively. The maximum magnetic field on the entire surface of the Earth invariably falls in the southern polar region, which imply that $B^S_{max} > B^N_{max}$. The decrease in the magnetic field at the average rate of ~12 nT/year in the southern polar region and ~25 nT/year in the northern polar region is apparent in Fig. 1(d) and (g). It may be noted that similar to the SAA region the magnetic field in the southern pole region is steadily decreasing since 1750. In Fig. 1(f) we have added 360 to westward longitudes (negative ϕ^S_{max}) to get the continuity in the longitudinal movement of B^S_{max}. Both Fig. 1(e) and (f) implies that this maximum magnetic field has moved northward from approximately 75°S to 65°S, and westward from 170° W to 140°E. The northward shift in the latitude is 0.1°/year and the westward shift in longitude is 0.25°/year. At 1000 km, the rate of decrease of B^S_{max} is slightly more at 15 nT/year and it is moving northward and westward at the rate of 0.08 °/year and 0.14 °/year, respectively. Its north-west movement at 1000 km is slower as compared to its movement on the surface of the Earth during 1840–2020. The most evident feature is both SAA and southern pole magnetic field regions are moving westward. Fig. 1(a-f) clearly indicate that magnetic field variation in SAA and southern pole regions are consistent in terms of variation in their strength and movement. However, for the northern polar region, such consistent behaviour is not seen (see Fig. 1i). Unlike SAA and southern polar regions, the location of B^N_{max} is not stable. During 1840–1940 the B^N_{max} was located close to $92^\circ - 98^\circ$W and $53^\circ - 57^\circ$ N, whereas during 1950–2020 there is a sudden shift in its location and it is located close to $102^\circ - 107^\circ$ E and $61^\circ - 62^\circ$ N. This sudden swift shift in the location of maximum magnetic field from Canadian sector to Siberia sector got attention of many researchers based on the recent reports (Witze, 2019; Livermore et al., 2020). The rapid acceleration of north pole is attributed to the magnetic flux expulsion from the core (Chulliat et al., 2010).

It may be noted that longitudinal westward drift of the SAA and southern pole regions is taking place at nearly the same rate. However, the SAA region is moving in the south-west direction and the southern pole region is moving north-west, and this behaviour is consistent at an altitude of 0 km and 1000 km as apparent in Fig. 2(a) and (b), respectively. While drifting south-west the trajectory of B_{min}, respectively makes an angle of approximately 8.3° and 5.1° with the west direction on the surface and at an altitude of 1000 km. Whereas, B^S_{max} is drifting in such a way that its trajectory makes an angle of approximately 19° and 27.7 with the west direction on the surface and at an altitude of 1000 km, respectively. Overall, we can see that in the SAA and both polar regions the magnetic field has steadily weakened over the last two centuries. As mentioned earlier, the SAA and southern pole regions are firm and show systematic time variation in their strength and location but for the northern pole region, there is a sudden shift in its location. Therefore, in all further detail analysis, we have examined the variation of the geomagnetic field from the SAA and southern pole region. Hereafter, we use the notations $\phi_{max} = \phi^S_{max}, \lambda_{max} = \lambda^S_{max}$ and $B_{max} = B^S_{max}$.

3.2. Longitudinal-latitudinal extent of SAA and southern pole regions

We have estimated the longitudinal and latitudinal extent of the SAA region. We took the longitudinal variation of the magnetic field at the latitude where B_{min} is located and compiled it for 1840–2020. The variation of $B(\lambda_{min}, \phi, t)$ during 1840–2020 is shown in Fig. 3(a). The location of B_{min} is marked by black dots in Fig. 3(a). The variation of $B(\lambda_{min}, \phi, t)$ clearly indicates the increase in longitudinal extent of SAA region. Similarly, we took the latitudinal variation of the magnetic field at the longitude where B_{min} is located and compiled it for the same period. The variation of $B(\lambda, \phi_{min}, t)$ during 1840–2020 is shown in Fig. 3(b). The tendency of an increase in the latitudinal width of the SAA region is apparent in 3(b). Similarly, we examined the longitudinal and latitudinal extent of B_{max} around the southern pole region. We took the longitudinal and latitudinal variation of the magnetic field around the location of B_{max} and compiled the data for 1840–2020. The variation of $B(\lambda_{max}, \phi, t)$ and $B(\lambda, \phi_{max}, t)$ are shown in Fig. 3(c) and (d), respectively. The location of B_{max} is marked by black dots in the lower panels of Fig. 3. The shrinking of the extent of the larger magnetic field region around B_{max} in southern polar region over 1840–2020 is apparent in Fig. 3(c) and (d). In Fig. 3(a,b) one can see that the blue color becomes darker, and in Fig. 3(c,d) the red color becomes lighter as we move towards 2020. Overall, it indicates a consistent weakening of the B_{min} in the SAA and B_{max} in the southern pole region over 1840–2020.

Next, we quantified the longitudinal and latitudinal extent of the SAA. We took the longitudinal and latitudinal profiles of the magnetic field at the location of B_{min}. As an example, for the year 2020, the longitudinal variation of the magnetic field at latitude λ_{min} and latitudinal variation of the magnetic field at longitude ϕ_{min} are displayed in Fig. 4(a) and 4(b), respectively. The red dots marked in these figures represent B_{min} for the year 2020. The two vertical dotted lines in Fig. 4(a) and 4(b) represent the locations where the magnetic field acquires the value of 1.2

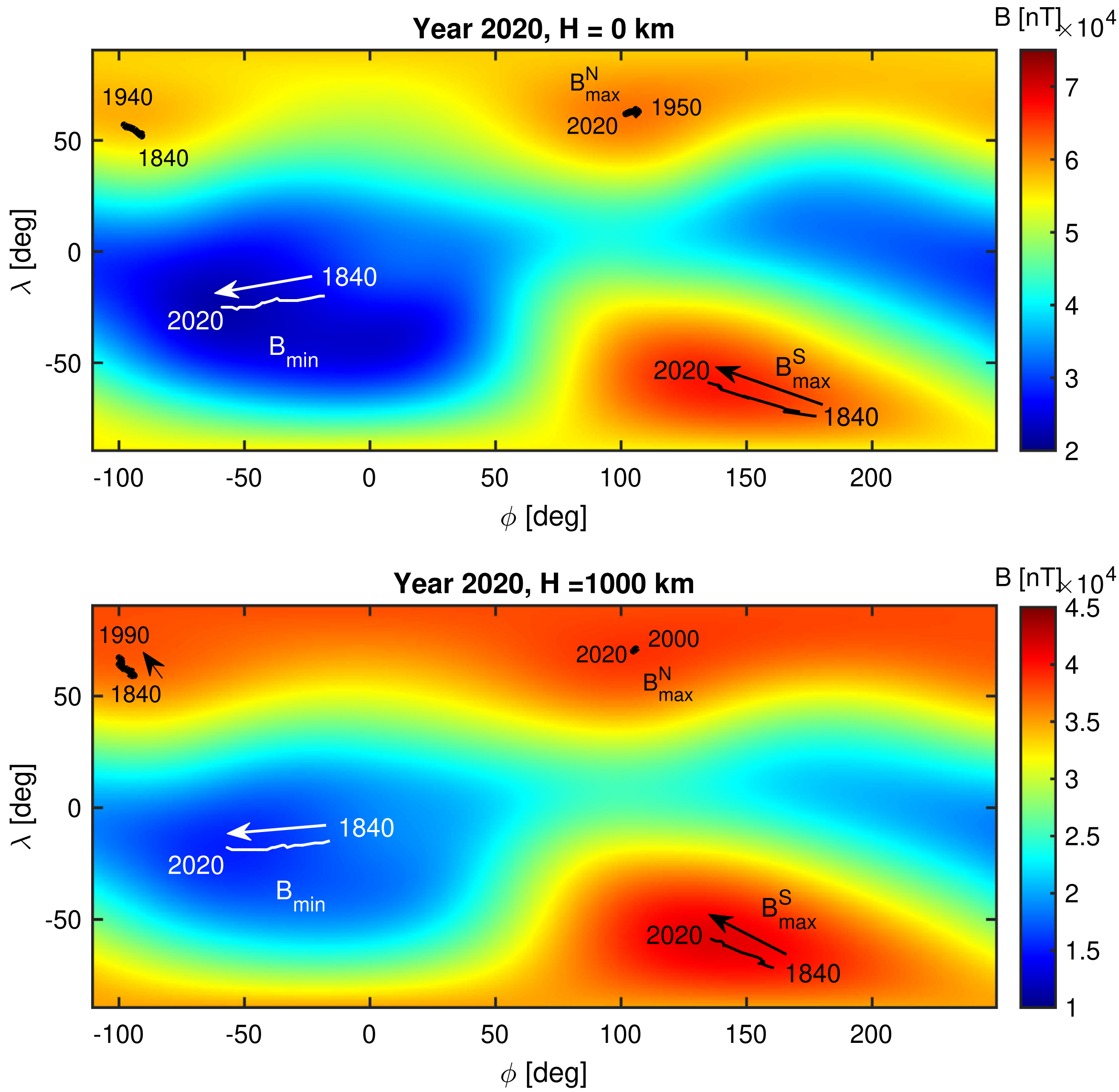

Fig. 2. This figure shows the movement of minimum magnetic field (in the SAA region) and maximum magnetic field (in the southern and northern polar region) (a) on the surface of the Earth and (b) at 1000 km altitude for the period of 1840–2020.

times of the B_{min} in the longitudinal and latitudinal direction. These positions of longitude and latitude are denoted by $[\phi_1, \phi_2]$ and $[\lambda_1, \lambda_2]$, respectively. The longitudinal and latitudinal extent is obtained by estimating the difference $\Delta\phi = \phi_2 - \phi_1$ and $\Delta\lambda = \lambda_2 - \lambda_1$, respectively. The variation of latitudinal extent, $\Delta\lambda$ and longitudinal extent $\Delta\phi$ is plotted as a function of time in Fig. 4(c) for altitude of 0 km (depicted by filled circles) and 1000 km (depicted by asterisk). The total longitudinal-latitudinal extent of the SAA region is computed from $\Delta\lambda \times \Delta\phi$ and shown in Fig. 4(d) for 0 km (depicted by red filled circles) and 1000 km (depicted by blue filled circles). Here, the total longitudinal-latitudinal extent represents the rectangular area around B_{min}, where the magnetic field has increased by 20% of the B_{min} in latitudinal and longitudinal directions at a given altitude. We noticed that the total longitudinal-latitudinal extent of the minimum magnetic field area varies in the range of 3300–4900 deg^2 on the surface, whereas it is in the range of 5000–5800 deg^2 at 1000 km altitude. On the surface, one deg^2 corresponds to $\approx$12321 km^2. It is seen that the longitudinal-latitudinal extent of minimum magnetic field area in the SAA region has increased steadily from 1920 to cover a rectangular area of 3360–4324 deg^2. The rate of increase of longitudinal-latitudinal extent is estimated to be 7.8 deg^2/year. At 1000 km, a similar trend is seen and it is found that the longitudinal-latitudinal extent is increasing at the rate of 5.4 deg^2/year. It may be noted that at a given time the longitudinal-latitudinal extent is higher at 1000 km as compared to that on the surface of the Earth. It is because at lower altitudes the magnetic field gradients are stronger, whereas at higher altitudes it is weaker. Therefore, at a higher altitude the location where the magnetic field increases by 20% of B_{min} is situated farther from the

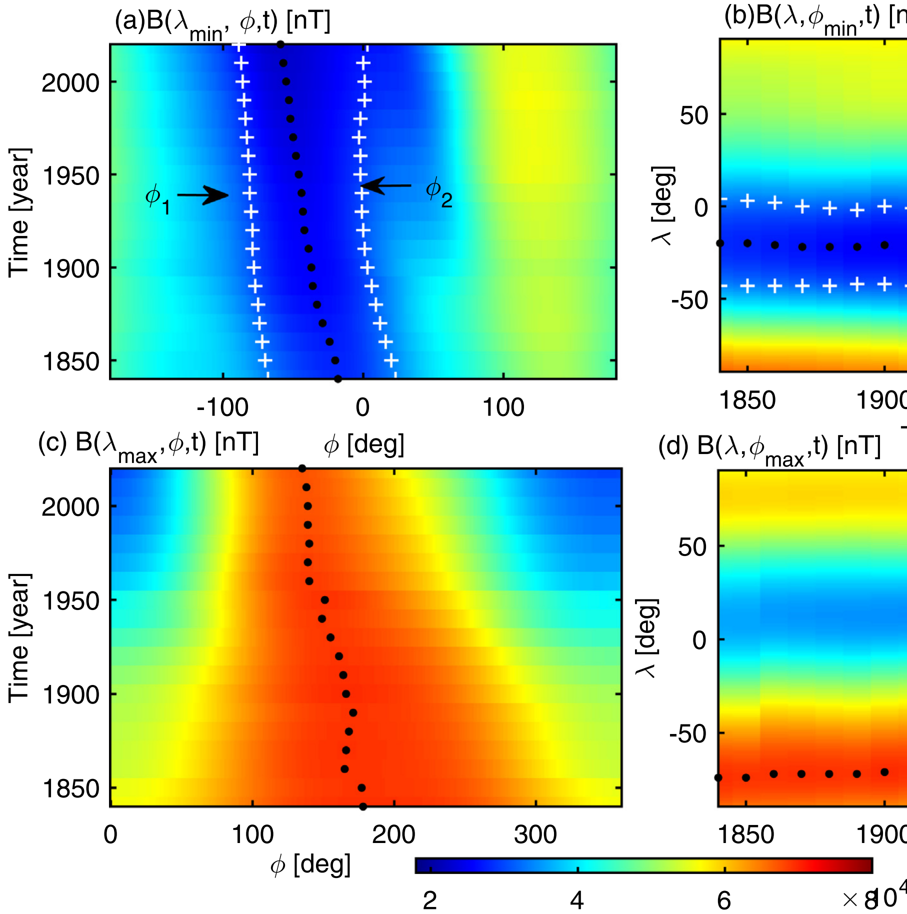

Fig. 3. The figure demonstrates the variation of (a) $B(\lambda_{min}, \phi, t)$ as a function of longitude, (b) $B(\lambda, \phi_{min}, t)$ as a function of latitude in SAA region and (c) $B(\lambda_{max}, \phi, t)$ as a function of longitude, (d) $B(\lambda, \phi_{max}, t)$ as a function of latitude in southern polar region during 1840–2020. These variations are on the surface of the Earth i.e. at 0 km altitude.

location of B_{min}. Whereas, at a lower altitude, they are situated closer to the location of B_{min} giving rise to lower values of $\Delta\lambda \times \Delta\phi$ on the surface as compared to that at 1000 km. We could not quantify the longitudinal-latitudinal extent of the south pole region as the magnetic field does not decrease by 20% around B_{max}. Increase in extent of SAA has been reported in recent studies (Amit et al., 2021). The dipolar field is decreasing with a rate of 12% per century, whereas the non-dipolar field is increasing with time at pronounced rate of 70% per century (Pavon-Carrasco and De Santis, 2016). This rapidly increasing non-dipolar magnetic field may contribute to observed increase in latitudinal-longitudinal extent of SAA.

3.3. Weakening of Earth's polar magnetic field

In the last two subsections, we have examined the movement of B_{min} and B_{max}, which basically gives information about a single point of 1° by 1° grid size. The analysis carried out in Section 3.1 indicated that the location of the maximum magnetic field in the northern polar region is not changing systematically and there is a sudden shift in its location. Thus, here we have examined the variation of the average magnetic field in entire polar regions. It will reflect the contribution from the magnetic poles as well as from nearby polar regions. In order to estimate the average magnetic field in the polar region, we have considered latitudinal zones; $66^\circ - 90^\circ$ in both the southern and northern hemispheres and estimated the average magnetic field by taking all values exceeding 40000 nT in those regions. This threshold is used to avoid contribution of SAA region to the estimated polar average magnetic field. This method is adopted from De Santis et al. (2012). The average magnetic field $\langle B \rangle$ for northern (blue) and southern (red) is shown in Fig. 5(a). The difference between the average polar magnetic field strength in the northern and southern hemisphere, $\delta = \langle B \rangle^N - \langle B \rangle^S$ is plotted as a function of time in Fig. 5(b). It may be noted that δ is negative from 1840 approximately until 1970. It implies that the southern polar average magnetic field strength was always stronger as compared to the northern polar average magnetic field strength. But over the past 50 years the magnetic field in the southern polar region has decreased considerably such that presently, it is weaker than the northern polar average magnetic field, which resulted in positive values of δ after 1970. If we monitor activity only during the past few

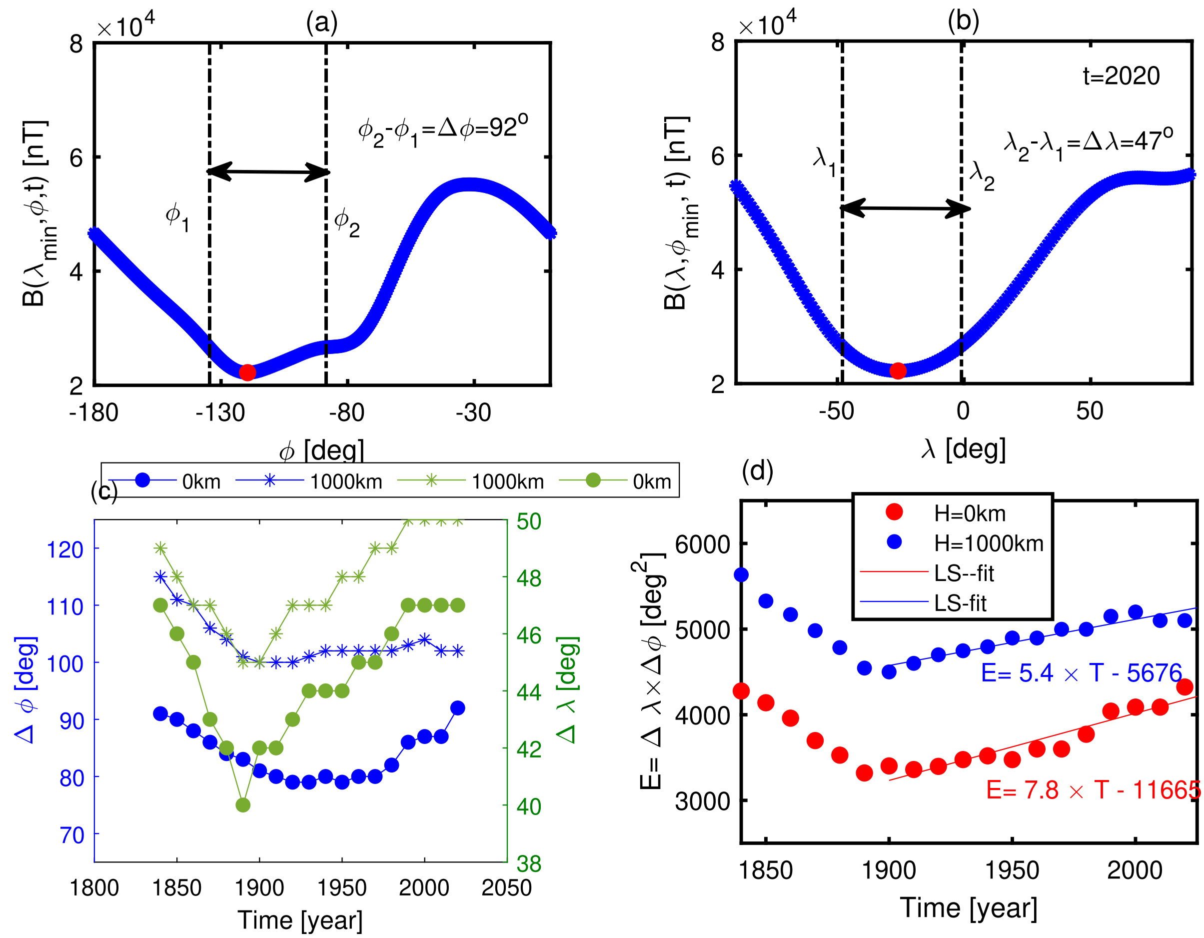

Fig. 4. The figure demonstrates (a) the longitudinal variation of magnetic field at λ_{min}, and (b) the latitudinal variation of magnetic field at ϕ_{min} in SAA for 2020 on the surface of the Earth ($H = 0$ km). The vertical dotted lines marked by $[\phi_1, \phi_2]$ and $[\lambda_1, \lambda_2]$ represents the location in longitudinal and latitudinal direction, where magnetic field reaches to a value of 1.2 times of the B_{min} (i.e., 20% increase in B_{min}). (c) The longitudinal ($\Delta\phi$) and latitudinal ($\Delta\lambda$) extent as a function of time for $H = 0$ km and $H = 1000$ km. (d) longitudinal-latitudinal extent of SAA around its minimum in deg^2 for $H = 0$ km and $H = 1000$ km.

decades (i.e., from 1950) then the rate of decrease of the average polar magnetic field in the southern polar region is 71 nT/year. Whereas, in the northern polar region the magnetic field has a slightly increasing trend with the rate of 9.5nT/year. This crossover in the strength of the southern and northern average magnetic fields is extremely important because it is a clear indication of the rapid weakening of the magnetic field in the southern polar region. It has direct implications to our ionospheric and neutral atmospheric dynamics in the southern polar and high-latitude regions (Tsurutani et al., 2016). This weakened polar magnetic field can affect the flux of energetic charged particles and cosmic rays entering the Earth's atmosphere and subsequently plays a crucial role in the long-term climate variations (Campuzano et al., 2018; Lanci et al., 2020). To understand the scenario on the entire globe we estimated the average magnetic field of the Earth by using the magnetic field information at each latitudinal and longitudinal grid of 1°. The average field of the Earth, $\langle B\rangle^{Earth}$ is plotted as a function of time in Fig. 5(c). It is evident that our planet is losing its magnetic field continuously over the past two centuries at the average rate of 26 nT/year.

3.4. Long-term trends in ground geomagnetic field observations

The analysis of the magnetic field obtained from the IGRF model clearly indicate the weakening of the Earth's magnetic field in the southern polar and SAA regions. To confirm this tendency with ground observations, we used magnetic field data from 15 stations listed in Table 1. These stations are marked on the globe in Fig. 6. As our interest lies in the long-term variation of the annual mean values of the magnetic field from these 15 stations are used as per data availability during the past few decades. Among these observatories, Syowa, and Dikson Island are not included in the IGRF model. There are a total of eight stations in the northern polar region (Group-C, numbered as 1 to 8), five stations are in the southern polar region (Group-B, numbered as 1 to 5), and two stations are in the SAA

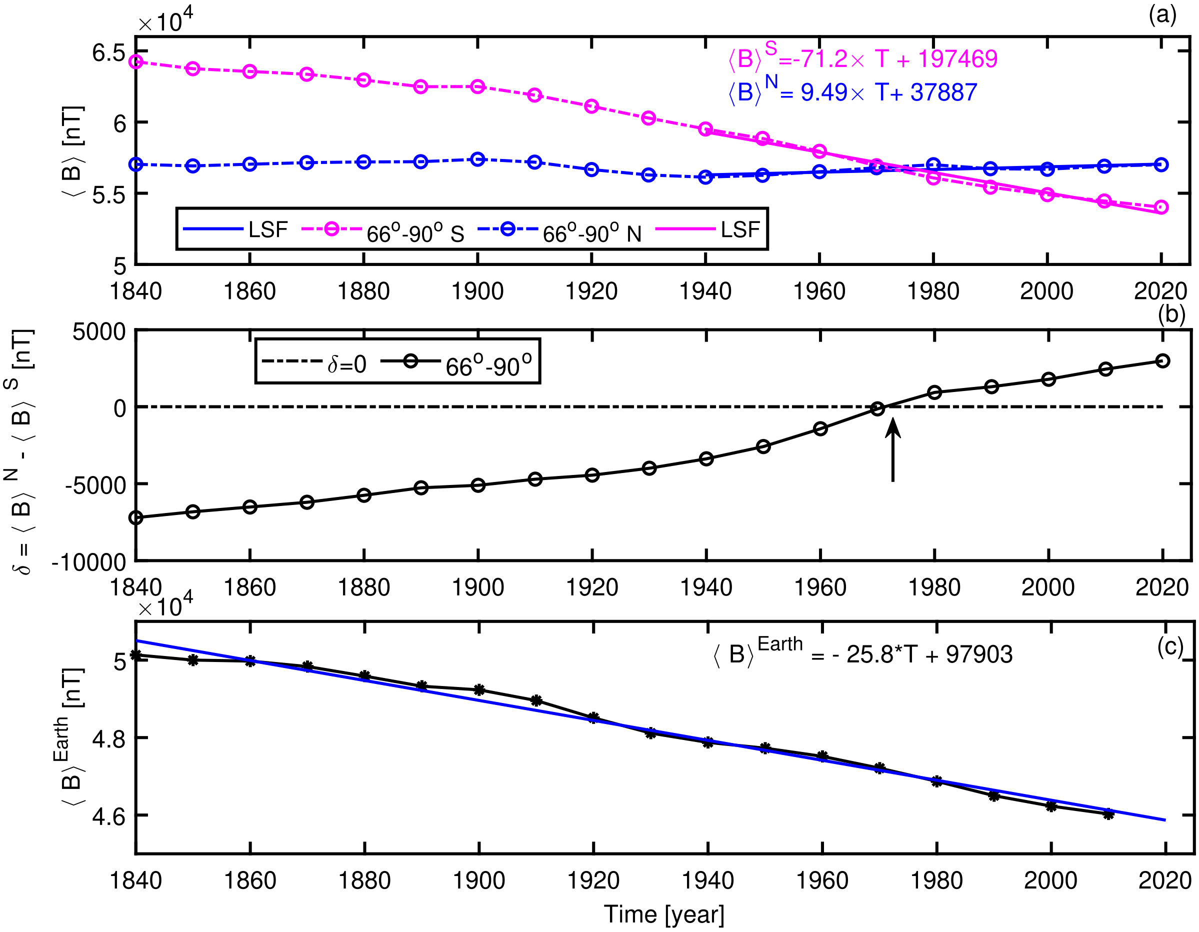

Fig. 5. This figure depicts (a) the average magnetic field $\langle B \rangle$ for northern (blue) and southern (magenta) hemisphere for latitudinal zones; $66^\circ - 90^\circ$. The variation of $\langle B \rangle$ from 1940–2020 is fitted with linear least square fit and equations are given. (b) The difference in the northern and southern average polar magnetic field strength as a function of time. (c) The time variation of the average field of the Earth, $\langle B \rangle^{Earth}$ since 1840.

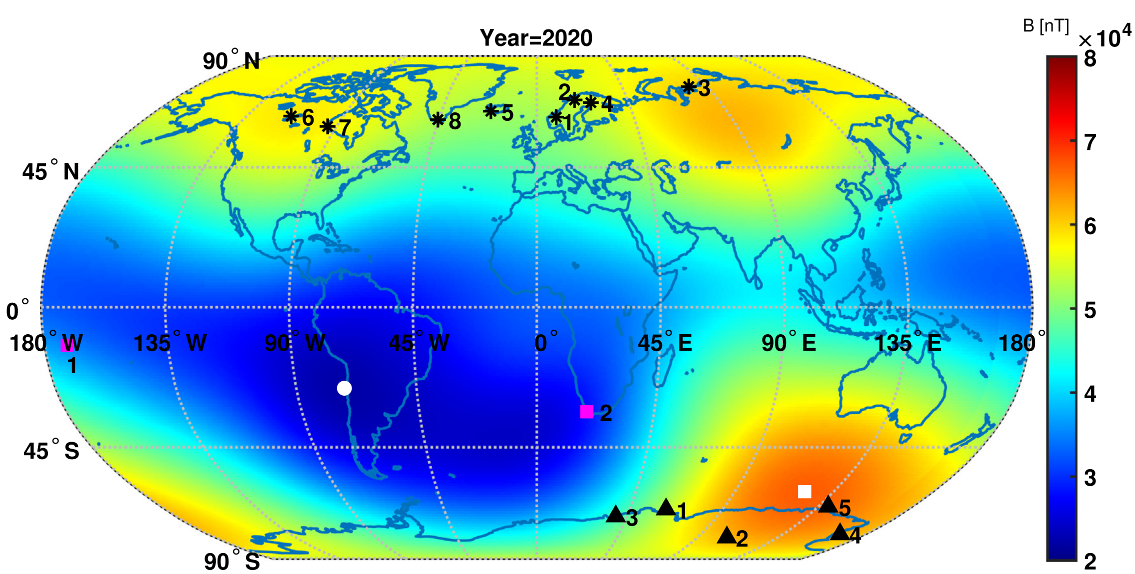

Fig. 6. There are a total of 8 stations in the northern polar region (numbered as 1 to 8 and marked by black asterisks), 5 stations in the southern polar region (numbered as 1 to 5 and marked by black triangles) and 2 stations in the SAA region (numbered 1 and 2 and marked by magenta squares). The current positions of B_{min} and B_{max} are marked with white circle and square, respectively.

region (Group-A, numbered as 1 and 2). This magnetic field data is provided by the British Geological Survey at http://www.geomag.bgs.ac.uk/. Let us first talk about the SAA region. We have shown the annual means of the magnetic field recorded at station Apia (API) and Hermanus (HER) in Fig. 7. The Apia and Hermanus stations respectively lie on the west-side and east-side of the longitude of the B_{min} in the SAA region. The decrease in the magnetic field at Apia and Hermanus in the SAA region is evident. The rate of decrease of the magnetic field at Hermanus is 98nT/year, which is larger as compared to Apia (i.e., 19nT/year). Whereas, B_{min} in SAA regions is decreasing at the rate of 31nT/year. This indicates that the magnetic field at Hermanus has decreased at a much faster rate in the recent past. It may be noted that B_{min} is located close to 25°S and 60°W, where the rate of decrease of the magnetic field is 30 nT/year, whereas Hermanus is situated in the SAA region but at 33°S and 19°E (i.e., right-side of the B_{min} location in the SAA). Recently, the possibility of splitting of SAA is reported (Rother et al., 2021). These authors have reported the second minimum in the SAA region located close to the 40°S and 1–2°E. It means the Hermanus station is rightly located close to the location of the second minima, which is presently emerging and it will become more distinct if the splitting process continues in the future. We attribute the higher rate of decrease of the magnetic field observed at Hermanus to the splitting of the SAA.

Similarly, the variation of the annual average of magnetic field strength observed at the eight observatories located in the northern polar region is shown in Fig. 8. In the northern polar region, we have observed two opposite tendencies. At five stations namely, Dombas (DOB), Abisko (ABK), Dikson Island (DIK), Sodankyla (SOD), and Leirvogur (LRV), the magnetic field shows increase at the rate of 18–28 nT/year over the past few decades. It may be noted that these observatories are located in the 22°W– 80°E longitudinal belt. Whereas, at Yellowknife (YKC), Fort Churchill (FCC) and Narsarsuaq (NAQ), which are located lies in the 46°W–115°W longitudinal belt, the magnetic field is decreasing at the rate of 21–75 nT/year. It means the magnetic field has consistently increased in one longitudinal belt and decreased at another longitudinal belt in the northern polar region. The scrutiny of the magnetic field from the observatories in the southern polar region namely, Mawson (MAW), Vostok (VOS), Syowa (SYO), Scott-base (SBA), and Dumont (DRV) indicate that magnetic field strength has decreased consistently in past few decades as evident in Fig. 9(a)-(e), respectively. All these stations lie in the longitudinal belt of 40°–167°E, which is close to the south pole. The decrease in the magnetic field in the southern polar region is clearly seen. The rate of decrease of the magnetic field is in the range of 35–72 nT/year. The average polar magnetic field obtained from the IGRF indicates a decrease of 78nT/year in the southern polar region, which is in agreement with the

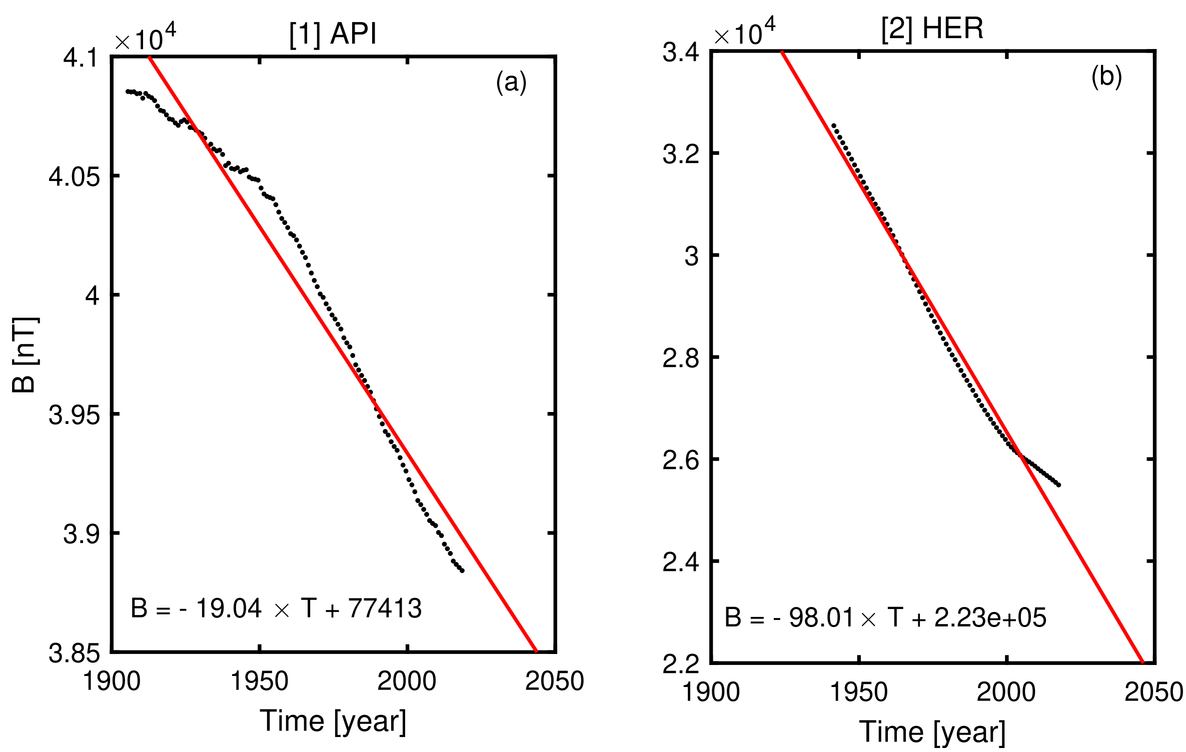

Fig. 7. This figure shows the variation of the annual average of the geomagnetic field at Apia [API] and Hermanus [HER] stations located inside the SAA region.

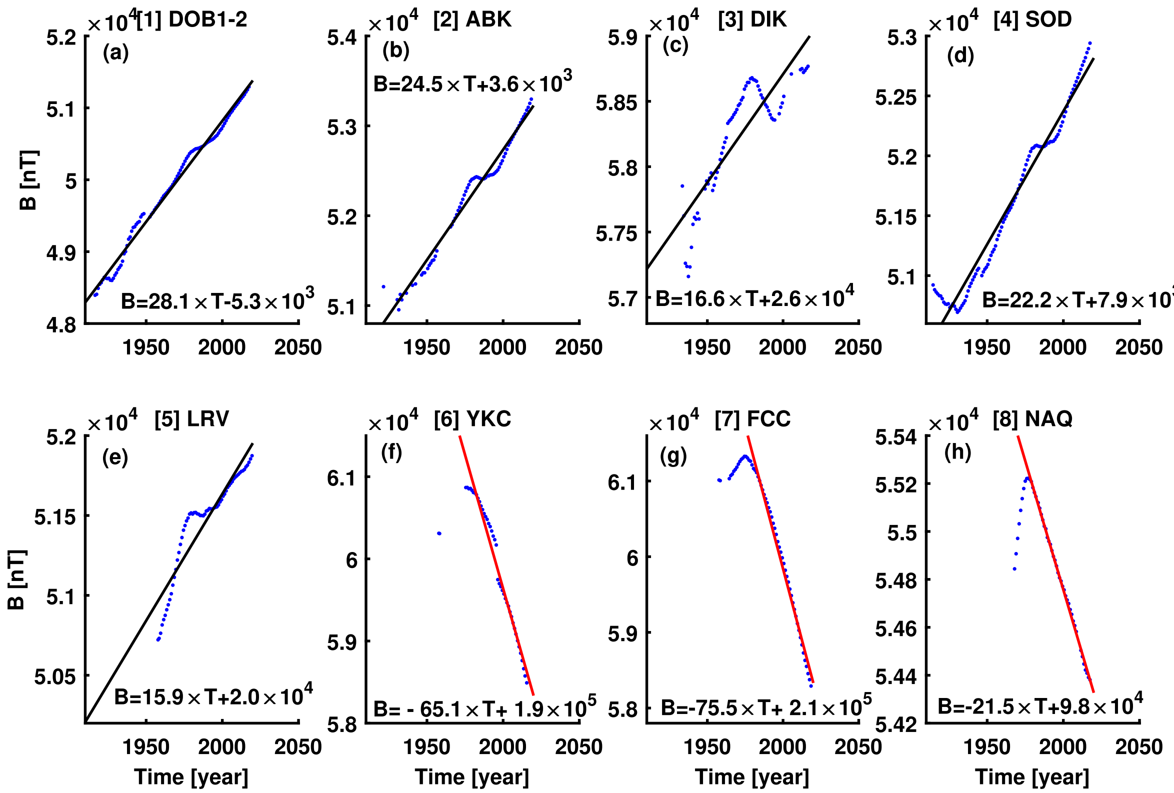

Fig. 8. The variation of the annual average magnetic field strength observed at eight magnetic observatories (Group-B) located in the northern polar region.

decrease observed at stations of these stations. We took all available magnetic field data for 1–8 stations in Group-C (northern polar region) and 1–5 stations in Group B (southern polar region) to estimate the average polar magnetic field of the Earth. The average polar magnetic field $\langle B \rangle$ estimated from the ground observations is plotted in Fig. 9(f). Here red curve is for the southern polar region and the blue curve is for the northern polar region. The tendency of crossover between the average northern and southern polar magnetic field is apparent. This tendency is discussed in the previous section using model data (see Fig. 5a).

3.5. Altitudinal variation of geomagnetic field

So far we have looked into latitudinal-longitudinal variation of magnetic field. In this section, we have examined the altitudinal variation of the geomagnetic field in the SAA and southern pole region. The examination of latitudinal-longitudinal-altitudinal variation of magnetic field provides three-dimensional information of magnetic field structure in the SAA region. Moreover understanding variation of magnetic field gradients in the latitudinal and longitudinal direction around the SAA center at different height is important as these magnetic field gradient affects the particle motions in the Earth's magnetosphere and it is important for the upcoming low earth orbiting satellite missions. As an example, the variation of the geomagnetic field at different altitudes for year 1900 and 2020 is presented in the form of video (see Supplementary Video S2 and S3). We obtained the minimum and maximum magnetic field and their location at every 200 km starting from the surface of the Earth up to 5000 km. The variation of $B_{min}, \lambda_{min}, \phi_{min}$ as a function of height is displayed in Fig. 10(a), (b) and (c), respectively. These variations are shown for two years namely, 1900 and 2010. Similarly, the variation of $B_{max}, \lambda_{max}, \phi_{max}$ as a function of height is displayed in Fig. 10(d), (e) and (f), respectively for year 1900 and 2010. Fig. 10 shows that the B_{min} and B_{max} both decreases with height. It means that the magnetic field strength in SAA and southern pole region decreases with height. It is expected as we know that magnetic field strength decreases as we move away from the source region. An interesting feature is that the location of B_{min} in the SAA region shifts in the north-east direction as we move to the higher altitudes (see Fig. 10b,c). In the southern pole region, a significant change in the latitude of the B_{max} location with respect to altitude is not observed. However, during the year 1900, the longitude of B_{max} location has changed considerably from 165° to 145°. Such change in location of B_{max} is not seen for the recent year 2020.

In order to get further information about the altitudinal structure of the SAA region, we have taken the latitudinal and longitudinal profile at the location of B_{min} at each altitude. As an example, for the year 1900, the plot of latitudinal profile and longitudinal profile of magnetic field

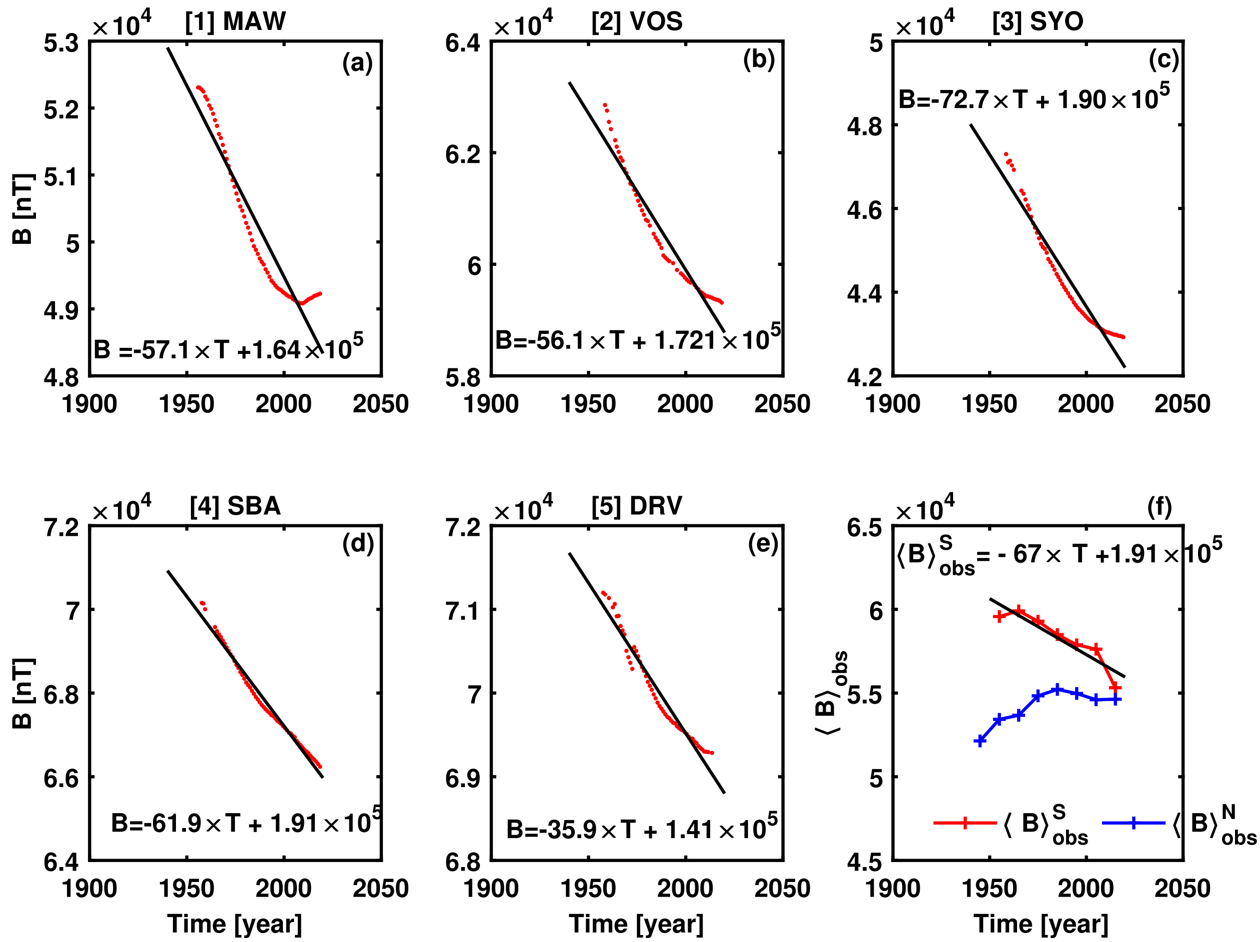

Fig. 9. The panels (a-e) shows the variation of the annual average magnetic field strength observed at the five magnetic observatories (Group-C) located in the southern polar region. The Panel (f) shows a variation of average magnetic field obtained from the magnetic field data recorded by the observatories located in the northern (blue) and southern (red) polar region provided in Table 1.

strength at the location of B_{min} is shown in Fig. 11(a) and (b), respectively for different altitudes. In Fig. 11(a) and (b), the magnetic field strength at a given altitude is normalized with the B_{min} at that altitude for comparison and better visualization. It means that normalized magnetic field strength B/B_{min} will always have a value of unity at the location of the minimum magnetic field at all altitudes. Therefore, the y-scale in Fig. 11(a) and (b) starts from one. We have marked a horizontal dashed-dotted line in 11(a) and (b) at B/B_{min}=1.2. The point of intersection of this horizontal line and latitudinal or longitudinal profiles indicate the location where the magnetic field increases by 20% of B_{min}. The variation of magnetic field strength across the latitudinal profile around B_{min} as a function of latitude and height is shown in Fig. 11(c), whereas its variation across the longitudinal profile as a function of longitude and height is shown in Fig. 11(d). In Fig. 11(c) and (d) the color bar indicates the magnetic field strength in log scale and the white dots indicate the movement of B_{min}. Fig. 11 clearly indicates that SAA is more structured at lower altitudes with steeper magnetic field gradients, whereas at higher altitudes it is less structured with shallower magnetic field gradients. In order to quantify the extent of SAA, we followed the method described in Section 3.2 and estimated $\Delta\phi, \Delta\lambda$, and $\Delta\lambda \times \Delta\phi$ of SAA at different altitudes for the years 1900 and 2020, which is shown in Fig. 12. We found that the extent in the longitudinal direction increases with height, whereas in $\Delta\lambda$ this tendency is not seen clearly. Overall the latitudinal-longitudinal extent of SAA, $\Delta\lambda \times \Delta\phi$ increases with height. As the magnetic field gradients are shallower at higher heights, the magnetic field varies slowly, and hence we have a wider extent of SAA at higher altitudes.

4. Summary and conclusions

In the present study, we have audited the variation of the geomagnetic field in the northern and southern polar regions, and the SAA region of the Earth by using the gufm1 + IGRF-13 model and 15 ground stations located in those regions. The rate of decrease of the geomagnetic field in the SAA and polar regions including the drift and extent of these regions are quantified at 0 km and 1000 km altitude above the surface of the Earth. The observed trends of decreasing magnetic field are validated with the ground observations. Apart from known SAA

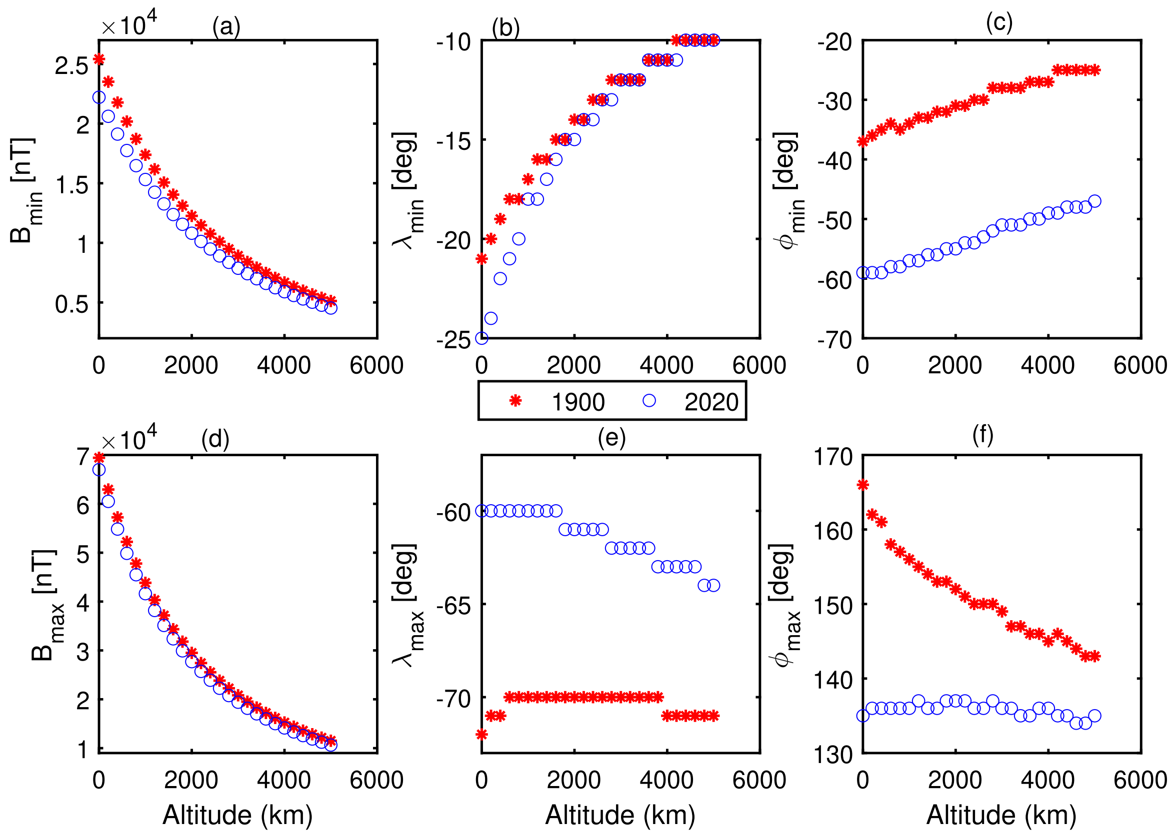

Fig. 10. This figure shows the variation of minimum magnetic field strength and associated latitude and longitude as a function of altitude in (a), (b), and (c), respectively. The variation of maximum magnetic field strength and associated latitude and longitude as a function of altitude in (d), (e) and (f), respectively. These variations are shown for two years 1900 (red) and 2020 (blue).

region (Amit et al., 2021) (≈ 50° E-130°W and 20°N-60°S), the consistent decrease in geomagnetic field is noted for the southern polar region (≈10°-180°E and 60°-80°S) over past two centuries. On the surface of the Earth, the rate of decrease of minimum (B_{min}), and maximum (B_{max}) magnetic field in the SAA and southern pole region are 30nT/year and 12nT/year, respectively. Whereas, at 1000 km these rates are 19nT/year and 15nT/year, respectively. Using the model the estimated rate of decrease of B_{min} in the SAA region is found to be 30nT/year. However, on the ground at Hermanus station, which falls in the SAA region, the rate of decrease of the magnetic field is noted as 98nT/year, which is significantly high. Such a significant decrease in the magnetic field could be associated with the phenomenon of splitting of the SAA reported by (Rother et al., 2021) as Hermanus station lies close to the location of the second minima in the SAA region.

The minima of the geomagnetic field in the SAA region and maxima of the geomagnetic field in the southern pole region are moving nearly at the same rate (≈ 0.22°-0.25°/year) in the westward direction. Overall, the SAA and southern polar regions are moving in the south-west and north-west direction such that it makes an angle of approximately 8.3° and 19° with west direction, respectively. The longitudinal-latitudinal extent $\Delta\lambda \times \Delta\phi$ around B_{min} in SAA region has increased steadily since 1920 at the rate of 7.8 degree^2/year. This tendency is also apparent at 1000 km altitude, where the extent of the SAA region is found to be increased steadily at the rate of 5.4 degree^2/year. We also found that the magnetic field gradients around the center of the SAA become shallower at higher altitudes.

Recently, Finlay et al., 2020 have presented the CHAOS-7 model of the time-dependent near-Earth geomagnetic field between 1999 and 2020 and observed changes in the South Atlantic Anomaly. This model is based on magnetic field observations collected by the low-Earth orbit satellites Swarm, CryoSat-2, CHAMP, SAC-C, and Ørsted, and on annual differences of monthly means of ground observatory measurements. This model shows that the South Atlantic weak field anomaly continues to expand and moves westward. Another, candidate field model for IGRF-13, the Mag.num.IGRF13 geomagnetic core field model (Rother et al., 2021), which is constrained by Swarm satellite and ground observatory data from November 2013 to August 2019 also shows the decreasing magnetic field in the SAA region and its westward movement. It implies that the trend of decreasing

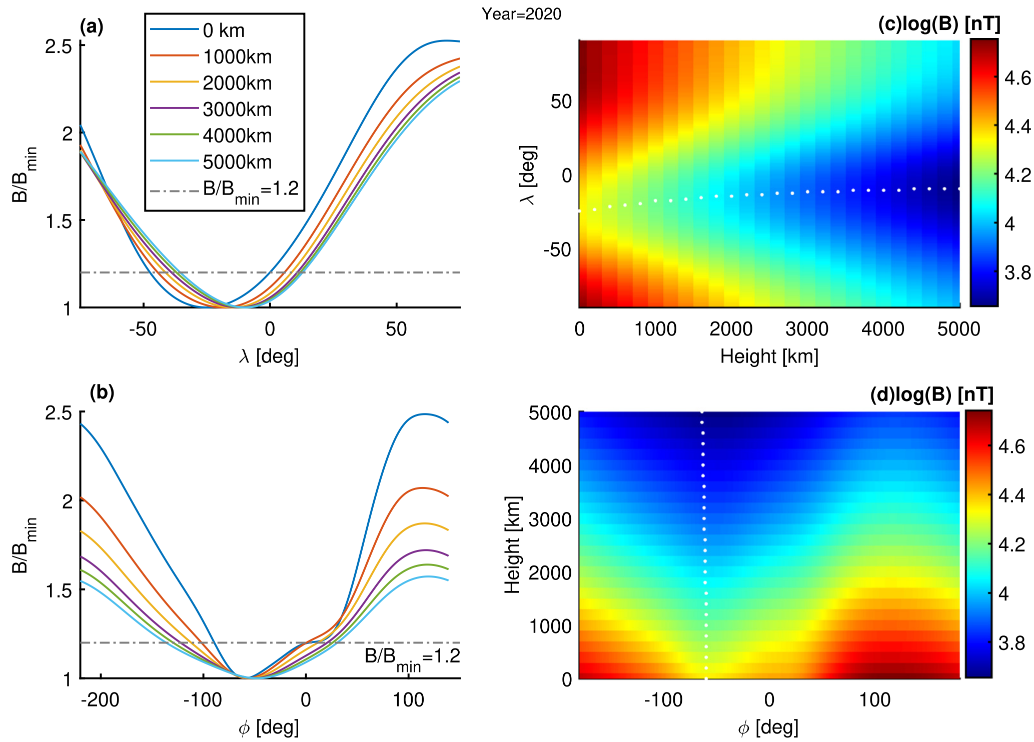

Fig. 11. For the year 2020, the variation of the magnetic field in (a) latitudinal direction and (b) longitudinal direction around the location of B_{min} is plotted for different altitudes. Here, the y-scale starts from one as we have a normalized magnetic field with the minimum magnetic field at that altitude. $B/B_{min} = 1$ indicate the location of B_{min}. The magnetic field variation in (c) latitudinal-altitudinal plane and (d) longitudinal-altitudinal plane at the location of B_{min}. Here, the color bar represents the magnetic field strength in the log scale.

magnetic field in the SAA region and its expansion over few decades is well supported by the recent satellite observations.

Another important feature is that the average magnetic field in the southern polar region (66°-90°) was invariably stronger as compared to the northern polar average magnetic field. But over the past fifty years, the magnetic field in the southern polar region has experienced a considerable decrease such that presently it is weaker than the average magnetic field in the northern polar region. Such cross-over in the average magnetic field in the polar region is apparent in the ground magnetic field observations as

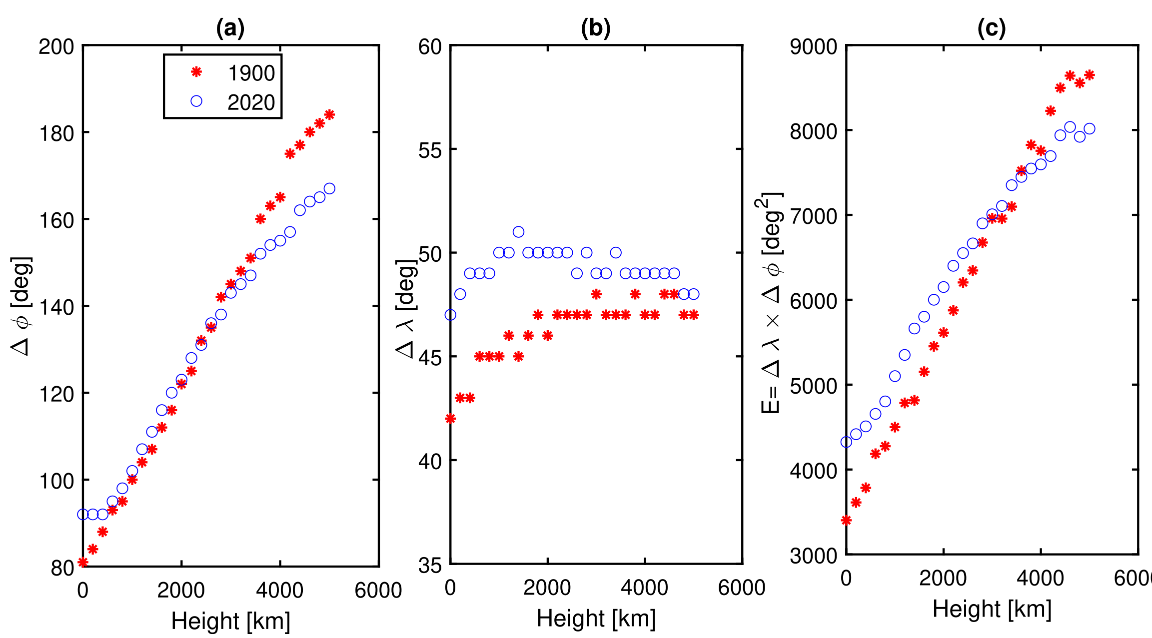

Fig. 12. For SAA region, the variation of (a) $\Delta\phi$ in degree (b) $\Delta\lambda$ in degree and (c) extent $\Delta\phi \times \Delta\lambda$ in $degree^2$ as a function of altitude is shown for the years 1900 and 2020.

well. In this period the rate of decrease of the southern polar average magnetic field is found to be 78nT/year, but such rapid decrease is not seen for the northern polar magnetic field. This hemispherical duality might be related to the asymmetry in the core field and its secular variation (Zossi et al., 2020). The polar magnetic field affects the polar cap and auroral oval. It has been shown that the areas of the polar cap and auroral oval have increased from 1940–2015 (Zossi et al., 2020). The strength of the geomagnetic field in those regions control the precipitation of energetic particles. The precipitation of energetic particles in a relatively confined region of the atmosphere is an important feature influencing the atmospheric dynamics (Tsurutani et al., 2016). Recent simulations indicate that the decrease of the geomagnetic field in the SAA region is causing energetic particles of the inner radiation belts to move steadily closer to the Earth (Soni et al., in press). These simulations showed that the radiation belt's lower boundary has moved approximately 434–590 kms closer to the Earth in the last 120 years (1900–2020). Increased radiation dose due to weakening of the magnetic field is dangerous to life and to our satellites. Thus, measuring geomagnetic field strength in polar and SAA regions and their monitoring essential.

Overall, our planet is losing its magnetic field continuously over the past 180 years at an average rate of 26 nT/year. It is suggested that this steady decay in the dipole magnetic moment is controlled by a planetary-scale gyre in the liquid metal outer core, and this decay may continue for the next few years (Finlay et al., 2016). The changing The Earth's magnetic field provides researchers new opportunities to understand the Earth's core, and how its dynamics influence other aspects of the Earth system. The models are the most preferred tools to study the global variation of magnetic field and to get prepared for the future challenges and hazards posed by the weakening of Earth's magnetic field we require highly accurate models. In this context, high-quality geomagnetic field data distributed evenly over the Earth's surface and high-resolution satellite data are therefore a fundamental prerequisite for the accurate model. A global plan of action to improving the spatial distribution of the geomagnetic observatories, the aeromagnetic and marine magnetic surveys to fill in the gaps, and low orbiting multi-satellites for the best spatial coverage are the essential elements for the development of the best futuristic IGRF models.

Declaration of Competing Interest

The authors declare that they have no known competing financial interests or personal relationships that could have appeared to influence the work reported in this paper.

Acknowledgement

We would like to acknowledge the use of data sets used in this work. The IGRF-13 model is provided by NGDC NOAA at www.ngdc.noaa.gov/geomag. The ground geomagnetic field data is provided by the British Geological Survey at http://www.geomag.bgs.ac.uk.

Appendix A. Supplementary material

Supplementary data associated with this article can be found, in the online version, at https://doi.org/10.1016/j.asr.2021.12.011.

References

Alken, P., Thebault, E., Beggan, C., Aubert, J., Baerenzung, J., Brown, W. J., Califf, S., Chulliat, A., Cox, G., Finlay, C.C., et al., 2021a. Evaluation of candidate models for the 13th generation international geomagnetic reference field. Earth Planets Space 73, 1–21. https://doi.org/10.1186/s40623-020-01281-4.

Alken, P., Thébault, E., Beggan, C.D., Amit, H., Aubert, J., Baerenzung, J., Bondar, T., Brown, W., Califf, S., Chambodut, A., et al., 2021b. International geomagnetic reference field: the thirteenth generation. Earth Planets Space 73, 1–25. https://doi.org/10.1186/s40623-020-01288-x.

Amit, H., Terra-Nova, F., Lézin, M., Trindade, R.I., 2021. Non-monotonic growth and motion of the south atlantic anomaly. Earth Planets Space 73, 1–10.

Brown, M., Korte, M., Holme, R., Wardinski, I., Gunnarson, S., 2018. Earth's magnetic field is probably not reversing. Proc. Nat. Acad. Sci. 115, 5111–5116. https://doi.org/10.1073/pnas.1722110115.

Cafarella, L., Lepidi, S., Meloni, A., Santarelli, L., 2009. Twenty years of geomagnetic field observations at mario zucchelli station (antarctica). Ann. Geophys. https://doi.org/10.4401/ag-4567.

Campuzano, S., De Santis, A., Pavón-Carrasco, F.J., Osete, M.L., Qamili, E., 2018. New perspectives in the study of the Earth's magnetic field and climate connection: The use of transfer entropy. PloS One 13, e0207270.

Campuzano, S.A., Gómez-Paccard, M., Pavón-Carrasco, F.J., Osete, M. L., 2019. Emergence and evolution of the South Atlantic Anomaly revealed by the new paleomagnetic reconstruction shawq2k. Earth Planet. Sci. Lett. 512, 17–26. https://doi.org/10.1016/j.epsl.2019.01.050.

Chulliat, A., Hulot, G., Newitt, L., 2010. Magnetic flux expulsion from the core as a possible cause of the unusually large acceleration of the north magnetic pole during the 1990. J. Geophys. Res. Solid Earth 115.

De Santis, A., Qamili, E., Spada, G., Gasperini, P., 2012. Geomagnetic south atlantic anomaly and global sea level rise: A direct connection? J. Atmos. Sol.-terrestrial Phys. 74, 129–135.

Domingos, J., Jault, D., Pais, M.A., Mandea, M., 2017. The South Atlantic Anomaly throughout the solar cycle. Earth Planet. Sci. Lett. 473, 154–163. https://doi.org/10.1016/j.epsl.2017.06.004.

Finlay, C.C., 2008. Historical variation of the geomagnetic axial dipole. Phys. Earth Planet. Inter. 170, 1–14.

Finlay, C.C., Aubert, J., Gillet, N., 2016. Gyre-driven decay of the Earth's magnetic dipole. Nat. Commun. 7, 1–8.

Finlay, C.C., Jackson, A., Gillet, N., Olsen, N., 2012. Core surface magnetic field evolution 2000–2010. Geophys. J. Int. 189, 761–781.

Finlay, C.C., Kloss, C., Olsen, N., Hammer, M.D., Tøffner-Clausen, L., Grayver, A., Kuvshinov, A., 2020. The chaos-7 geomagnetic field model and observed changes in the south atlantic anomaly. Earth Planets Space 72, 1–31. https://doi.org/10.1186/s40623-020-01252-9.

Finlay, C.C., Maus, S., Beggan, C., Bondar, T., Chambodut, A., Chernova, T., Chulliat, A., Golovkov, V., Hamilton, B., Hamoudi, M., et al., 2010a. International geomagnetic reference field: the eleventh generation. Geophys. J. Int. 183, 1216–1230. https://doi.org/10.1111/j.1365-246X.2010.04804.x.

Finlay, C.C., Maus, S., Beggan, C.D., Hamoudi, M., Lowes, F.J., Olsen, N., Thébault, E., 2010b. Evaluation of candidate geomagnetic field

models for igrf-11. Earth Planets Space 62, 787–804. https://doi.org/10.5047/eps.2010.11.005.
Garnero, E.J., McNamara, A.K., 2008. Structure and dynamics of Earth's lower mantle. Science 320, 626–628. https://doi.org/10.1126/science.1148028.
Girgis, K.M., Hada, T., Matsukiyo, S., 2020. Solar wind parameter and seasonal variation effects on the South Atlantic Anomaly using Tsyganenko models. Earth Planets Space 72, 1–17.
Gubbins, D., Jones, A.L., Finlay, C.C., 2006. Fall in earth's magnetic field is erratic. Science 312, 900–902.
Hartmann, G.A., Pacca, I.G., 2009. Time evolution of the South Atlantic Anomaly. Anais da Academia Brasileira de Ciências 81, 243–255.
Jackson, A., Jonkers, A.R., Walker, M.R., 2000. Four centuries of geomagnetic secular variation from historical records. Philos. Trans. R. Soc. Lond. Ser. Math. Phys. Eng. Sci. 358, 957–990.
Kakad, B., Kakad, A., 2020. Characteristics of probability distribution functions of low-and high-latitude current systems during solar cycle 24. Adv. Space Res. 65, 1559–1567.
Kakad, B., Kakad, A., Ramesh, D.S., Lakhina, G.S., 2019. Diminishing activity of recent solar cycles (22–24) and their impact on geospace. J. Space Weather Space Clim. 9, A1.
Lanci, L., Galeotti, S., Grimani, C., Huber, M., 2020. Evidence against a long-term control on Earth climate by galactic cosmic ray flux. Global Planet. Change 185, 103095.
Livermore, P.W., Finlay, C.C., Bayliff, M., 2020. Recent north magnetic pole acceleration towards siberia caused by flux lobe elongation. Nat. Geosci. 13, 387–391.
Lowes, F., 2000. An estimate of the errors of the igrf/dgrf fields 1945–2000. Earth Planets Space 52, 1207–1211.
Molinski, T.S., Feero, W.E., Damsky, B.L., 2000. Shielding grids from solar storms [power system protection]. IEEE Spectr. 37, 55–60.
Pavon-Carrasco, F.J., De Santis, A., 2016. The South Atlantic Anomaly: The key for a possible geomagnetic reversal. Front. Earth Sci. 4, 40. https://doi.org/10.3389/feart.2016.00040.
Rajaram, G., Arun, T., Dhar, A., Patil, A., 2002. Rapid decrease in total magnetic field F at antarctic stations-its relationship to core–mantle features. Antarct. Sci. 14, 61–68. https://doi.org/10.1017/S0954102002000585.
Rother, M., Korte, M., Morschhauser, A., Vervelidou, F., Matzka, J., Stolle, C., 2021. The mag. num core field model as a parent for igrf-13, and the recent evolution of the south atlantic anomaly. Earth Planets Space 73, 1–17. https://doi.org/10.1186/s40623-020-01277-0.
Schaefer, R., Paxton, L., Selby, C., Ogorzalek, B., Romeo, G., Wolven, B., Hsieh, S.-Y., 2016. Observation and modeling of the South Atlantic Anomaly in low Earth orbit using photometric instrument data. Space Weather 14, 330–342. https://doi.org/10.1002/2016SW001371.
Soni, P.K., Kakad, B., Kakad, A., in press. Deepening of radiation belt particles in south atlantic anomaly region: A scenario over past 120 years. Adv. Space Res (in press).
Tarduno, J.A., Watkeys, M.K., Huffman, T.N., Cottrell, R.D., Blackman, E.G., Wendt, A., Scribner, C.A., Wagner, C.L., 2015. Antiquity of the South Atlantic Anomaly and evidence for top-down control on the geodynamo. Nat. Commun. 6, 1–6. https://doi.org/10.1038/ncomms8865.
Tsurutani, B., Hajra, R., Tanimori, T., Takada, A., Remya, B., Mannucci, A., Lakhina, G., Kozyra, J., Shiokawa, K., Lee, L., et al., 2016. Heliospheric plasma sheet (HPS) impingement onto the magnetosphere as a cause of relativistic electron dropouts (REDs) via coherent EMIC wave scattering with possible consequences for climate change mechanisms. J. Geophys. Res. Space Phys. 121, 10–130.
Tsurutani, B.T., Gonzalez, W., Lakhina, G., Alex, S., 2003. The extreme magnetic storm of 1–2 september 1859. J. Geophys. Res. Space Phys. 108.
Wang, W., Liu, J., Zhu, F., Li, M., Dorfman, S.M., Li, J., Wu, Z., 2021. Formation of large low shear velocity provinces through the decomposition of oxidized mantle. Nat. Commun. 12, 1–10. https://doi.org/10.1038/s41467-021-22185-1.
Witze, A., 2019. Earth's magnetic field is acting up and geologists don't know why. Nature 565, 143–145. https://doi.org/10.1038/d41586-019-00007-1.
Zossi, B., Fagre, M., Amit, H., Elias, A.G., 2019. Polar caps during geomagnetic polarity reversals. Geophys. J. Int. 216, 1334–1343. https://doi.org/10.1093/gji/ggy494.
Zossi, B., Fagre, M., Amit, H., Elias, A.G., 2020. Geomagnetic field model indicates shrinking northern auroral oval. J. Geophys. Res. Space Phys. 125. https://doi.org/10.1029/2019JA027434, e2019JA027434.